Research Square

Preprints are preliminary reports that have not undergone peer review.
They should not be considered conclusive, used to inform clinical practice,
or referenced by the media as validated information.

# Extreme Winds Flip Influence of Fuels and Topography on Megafire Burn Severity in Mesic Conifer Forests Under Record Fuel Aridity

**Cody Evers** ( cevers@pdx.edu )
Portland State University
**Sebastian Busby**
Portland State University
**Max Nielsen-Pincus**
Portland State University
**Andrés Holz**
Portland State University

**Research Article**

**Keywords:** Wildfire, Oregon Labor Day fires, Western Cascades, High-severity fire, Climate-limited fire regime, Megafires.

**Posted Date:** July 8th, 2021

**DOI:** https://doi.org/10.21203/rs.3.rs-654932/v1

**License:** This work is licensed under a Creative Commons Attribution 4.0 International License.
Read Full License

# Abstract

The coupling of unusually hot and dry weather have led to global increases in the occurrence of megafires. Despite the conventional wisdom that extreme heat and aridity overwhelm the controls on burn severity patterns (i.e., vegetation mortality), we hypothesize that wind is the main driver of megafire events in temperate mesic forests with climate-restricted fire regimes, yet that fuels and topography remain important influences on burn severity patterns. The infrequent occurrence of large high-severity wildfire in these forests means that contemporary empirical data (e.g., remote sensing) from past megafires are largely missing. During the extraordinary 2020 fire season, ca. 0.8 million ha burned in the North American Pacific Northwest (PNW) over two weeks under record-breaking fuel aridity and winds, representing the first modern example of megafires that characterize disturbance regimes west of the region's Cascade Mountains. Considering increasing concern and uncertainty surrounding the drivers of megafire events in temperate mesic forests, our objective was to understand the relative influence of, and potential interactions between, weather, fuels, and topography on high-severity (> 75% tree mortality) fire probability among five synchronous megafires in the western Cascade Mountains. To assess the influence of several potential drivers of high-severity fire and whether these relationships varied with land use and ownership, we developed remotely sensed fire extent and burn severity maps for two periods of the explosive 2020 PNW fire season: (1) during extreme winds and (2) after the extreme winds subsided. The area burned during the windstorm accounted for 90% of the total fire sizes and saw a 2.5-times greater proportion of high-severity fire than during the period without winds. Our results suggest that wind is the major driver of megafires in forests with climate-limited fire regimes, yet that fuels and topography shape burn severity patterns even under extreme fuel aridity and winds. The relative influence of topography on burn severity outweighed fuels during the windstorm, while fuels outweighed the influence of topography after winds subsided. Early-seral forests primarily concentrated on private lands, burned more severely than their older and taller counterparts, regardless of topography, over the entire megafire event. Meanwhile, mature stands burned severely only under extreme winds and especially on steeper slopes. Although climate change and land-use legacies may prime mesic temperate forests to burn more frequently and at higher severities than historically observed, and especially among early-seral forests, our work suggests that future high-severity megafires are only likely to occur during coinciding periods of heat, fuel aridity, and extreme winds.


# Significance

There is concern that megafires have been increasing in frequency globally due to changes in climate and land use, yet the immediate drivers of these events are poorly understood, especially in fuel-rich wet forests. Globally, these forests have burned infrequently in modern history and are a substantial source of ecosystem services. In September 2020, ca. two-thirds of a million hectares burned in the Pacific Northwest of North America, with a third of a million hectares of temperate mesic forests burned under very extreme weather conditions in western Oregon, USA alone resulting in unprecedented human impacts ranging from the loss of human lives to the loss of physical and cultural values (e.g. homes,

water supply systems, recreational sites, etc.). We examined the influence of fuels and topography on burn severity patterns and how influence changed during and after an extreme wind event. We found that fuels and topography influence burn severity patterns to a greater degree than previously recognized under extreme fire weather conditions. Given an ignition source, megafires in fuel-rich temperature forests are unlikely to take place without the co-occurrence of extreme wind, heat, and fuel aridity. Expanding fire season length under climate change, however, may increase the likelihood that strong wind events co-occur with extreme fuel aridity, ultimately driving an increasing frequency of megafire events.

# 1. Introduction

Megafires have surged globally (1–3) due to increasing and seasonally prolonged aridity (4–8), and which extensive impacts on carbon storage, radiative forcing, biodiversity, and ecosystem services (e.g., (9–12)). Ecosystems with climate-restricted fire regimes may be particularly sensitive to changes in aridity (13–16). These fire regimes, where long periods (> 100–300 years) of quiescent fire activity area are punctuated by episodic, regional-scale fire events (17, 18), are common within mesic, temperate forests, including those found in Eurasia, Southern Chile, SE Oceana, and in North America in the subalpine Rocky Mountains and the Pacific Northwest (PNW) (19–25), all of which have experienced megafires during the 2016–2020 period (26). While mesic, temperate forests compose only a fraction of the global temperate forest biome, they represent some of the most carbon-dense locations on the planet (27) and highly valued for their productivity. Empirical data of the effect of climate change on megafires in mesic forests remains equivocal, due largely to the inherent difficulty in studying these fire regimes (28–31) and the confounding influence of past and ongoing forest management (32, 33). A better understanding of the controls of fire extent and severity in mesic forests under extreme fire conditions is critical towards anticipating and adapting to the social and ecological impacts of fires on a warming planet.

The frequency and timing of megafires are linked to spatial and temporal variations and timing in biomass, flammability, extreme weather, and ignitions. Fluctuations among these controls determine how individual fire events unfold and over extended periods the size-frequency distribution that characterize different types or regimes of fire (34). The least active control will typically have the greatest influence on variation in fire activity for a given fire regime (35). In the case of fuel-rich mesic forests, fire regimes are strongly tied to regional-scale variations in climate and weather that can prime entire regions for megafire events (36–38). Synoptic-scale weather events have been shown to overwhelm the influence of fine-scale factors (34, 39, 40) such as topography (e.g., slope, aspect, heat load, and topographic wetness) and vegetation structure (e.g., stand age and canopy height) (41–43), which has contributed to the common assumption that vegetation and topography have limited influence on the extent and severity of fire events in infrequent high-severity fire regimes (39, 44, 45). Nonetheless, evidence to support this assumption is equivocal (e.g. (42, 46)).

In 2020, megafires burned ca. 4.1 M ha across the states of California, Oregon, and Washington, USA. In Oregon alone, 5 megafires west of the Cascade mountain range burned more area than fires in the

previous half-century combined and is likely one of the most extensive fire seasons across the region since Euro-American settlement (17, 20, 47, 48). Building off the hottest meteorological summer (June through August) on record in the Northern Hemisphere, the Labor Day fires occurred during the second driest year on record for the western US and during a strong drying east wind event that occurred throughout the Pacific Northwest region of the USA, including Oregon and Washington (48). Separately, these extreme climate and weather conditions were not unpresented, but when combined, broke instrumental records (38). While these fires are comparable to historical observations (49–51), no satellite records exist for these past disturbance events (47). The 2020 Labor Day fires in Oregon provide the first opportunity of its kind to quantitatively test the effects of wind and landscape conditions, such as topography and fuel characteristics, on megafire extent and severity patterns under extreme fuel aridity in mesic, fuel-rich temperature forests.

We developed extent and burn severity maps for the five megafires (ca., 335,000 ha) to empirically predict, rank, and compare the relative influence of fuels and topography on high burn severity probability (i.e., > 75% tree mortality) under record-breaking fuel aridity and variable wind conditions. We take advantage of the two distinct weather periods to examine how record fuel aridity and extreme winds interacted with fuels and topography to influence the probability of high burn severity across all five megafires. The first period (P1) was characterized by dry east winds and extreme atmospheric aridity; the subsequent period (P2) by calm west winds and lower atmospheric aridity yet sustained extreme fuel aridity. Specifically, we ask: (1) Do fuels or topography influence high-burn severity patterns when extreme fuel aridity is compounded with extreme and dry winds? (2) Do these relationships change during periods of extreme fuel aridity without winds? (3) How do interactions between fuels and topography shape high-burn severity patterns with and without extreme winds? and (4) How are high-burn severity patterns in P1 vs. P2 affected by the forest and fuel conditions resulting from past management practices?

We evaluated how the probability of high-burn severity varied between the 2 periods with regards to topographic and fuel structure variables associated with forest fire spread and burn severity, including stand age and canopy height (i.e., fuel structure; (17, 52)), slope and aspect (i.e., topography; (17)), and topographic indices of microclimatic fuel aridity (i.e., indices of topographic wetness and heat load; (53–55). We hypothesized that (1) fuels would have less impact than topography on burn severity during period P1 due to extreme winds, (2) that topography would remain the strongest predictor of high-severity patterns during P2, (3) that interactions between fuels and topography and high-burn severity would differ during P1 and P2, and (4) that management legacies associated with land ownership would be most pronounced during period P2 due to the lack of wind-driven fire spread. This work provides context and reference for ongoing discussions regarding preparedness and responses to megafires in mesic and fuel-rich ecological systems with climate-restricted wildfire regimes (e.g., (56, 57)).

# 2. Results

The five analyzed megafires burned 334,000 hectares total (Table S2), most of which (94%) occurred in upland mesic, conifer forests west of the Cascade crest. The vast majority of fire growth (90%) occurred

during the ca. 72-hr period between September 7th and 9th (P1), with the remainder occurring between September 10th and 16th once windspeeds had subsided but fuel aridity remained extreme (P2; Fig. 1; Table S2). The proportion of the area burned at high severity during the wind event was 2.5 times that of the period that followed (65% vs 26%; Table S3; Fig. S2) and accounted for ca. 57% of the total burned area of all five events – all areas likely to have > 75% tree mortality. The extent of high-severity fire differed proportionally among the five analyzed fires, ranging from 47.5–72.1%, and was inversely correlated with latitude (Table S3). The exception was the easternmost Lionshead Fire, which was the only fire to partially burn east of the Cascade crest, occurred at a higher elevation, and had the lowest proportional extent of high burn severity.

The importance of variables explaining high-burn severity probability differed during P1 and P2 (Fig. 2). Topographic effects related to micro-topography were most pronounced during the extreme wind and fuel aridity of P1 (i.e., ca. 65% of the contribution importance): slope was most important (28%, SD = 2%), followed by canopy height (22%, SD = 1.5%), aspect (18%, SD = 1.4%), TWI (13%, SD = 1.2%), stand age (13%, SD = 1.4%), and HLI (6%, SD = 1.3%). Under extreme winds and high fuel aridity, severity increased monotonically with slope, such that the probability of high burn severity was 50% higher on slopes greater than 30 degrees when compared to flat terrain (Fig. 2).

Outside of changes in importance, the relationships between fuel structure, topography, and the probability of high-burn severity changed substantially between the two periods (Fig. 2). During P2, and in contrast to hypothesis H2, under extreme fuel aridity but weak winds, the most important predictor of severity was fuel characteristics, with canopy height as the most important (32%), followed by stand age (17%), slope (16%), aspect (12%), HLI (12%), and TWI (11%). The probability of high-burn severity on east- and south-east-facing slopes was particularly pronounced during P1, whereas during P2 the influence of slope on high-burn severity probability was relatively homogenous across aspects (except for NW-facing slopes). The probability of high-burn severity changed during and after the windstorm event in areas from moderately high and low (although affecting a relatively small total area) to mostly just low topographic wetness (TWI). The influence of slope declined substantially once winds subsided during P2. The effect of heat load (HLI) was more pronounced during P2, where higher HLI values were positively associated with increased high-burn severity probability.

Forest fuel structure was important during both periods, with a greater influence on the probability of high-burn severity during P2 (ca. 49% of the contribution importance, contrary to hypothesis H2). During both burning periods, burn severity was in general negatively associated with canopy height. During P1, a bimodal response in high-burn severity probability was observed at ca. 8m and 33m in canopy height (Fig. 2). During P2, forest stands less than 10m in height were nearly 2x to 3x more likely to burn at high severity compared to those 20m in height or more (Fig. 2). During P1, a greater proportion of high severity was observed in early-seral (ca. 0–40 year) and late-seral (ca. 200–400 year) stands.

Interactions among fuel structure and topography showed non-linear behaviors and substantial differences between P1 and P2, supporting hypothesis H3. Of the four variable pairs with the greatest

interactions during both periods (Fig. 3), three involved slope, two involved canopy height, and two involved topographic wetness. Slope mediated the response among fuel structure and other topographic variables (Fig. 3). The most pronounced interaction - slope and canopy height - revealed that the probability of high-burn severity increased with decreasing canopy height and increasing slope. In these interactions, moderate to steep slopes had an amplifying effect on severity during P1, while flat slopes tended to have a dampening effect; during P2, very tall stands (> 40m) appeared buffered from the high-burn severity amplifying effect of slope. The probability of high severity was substantially higher at canopy heights less than 10m (Fig. 2, 3). Severity responses were relatively similar during P2 in the cases of slope and canopy height, but interactions differed among other pairs of explanatory variables, e.g., wetter topographic settings (higher TWI values) were protected even when dominated by short-stature forest (Fig. 3).

Two-thirds of the area burned occurred equally on private industrial timberlands and on adjacent national forest, while the remainder was found in a mixture of BLM timberlands, state forests, and private non-industrial lands (Table S4). High-burn severity patterns affected by the forest and fuel conditions resulting from past management practices varied by fire event, but private lands experienced the highest proportion of high-severity fire in 3 out of the 5 megafires analyzed here (Table S5). During P1 the ratios between observed and expected (based on available land) patterns of high-burn severity were similar under each ownership (i.e., forest fuel structures, including canopy height, stand age) (Fig. 4). As hypothesized, forest structure played a more important role during P2 and private industrial lands experienced a higher portion of high-burn severity compared to public. Early-seral forests with relatively short canopy heights (< 10m) also experienced disproportionately larger high-burn severity extent under both P1 (+ 26%) and P2 (+ 111%) periods (Fig. S3). These short early-seral forests were primarily concentrated on private (87%) versus public lands (13%).

# 3. Discussion

Our study contributes to the understanding of how wind, topography, and vegetation structure control megafire behavior and spread in mesic temperate forests. Specifically, we identified important changes in the relative influence of fuels and topography on the probability of high-severity fire within five western Cascade megafires under record fuel aridity, with and without extreme winds. While conceptual frameworks describing the relative influence of climate, weather, fuels, and topography on fire behavior and spread have been proposed in drier/warmer ecosystems in North America (58, 59) and elsewhere (23, 60, 61), our study advances understanding of how these factors interact at fine-scales to drive megafire events in mesic, biomass-rich, temperate forests with historically infrequent fire. Despite the conventional wisdom that extreme fire weather overrides the influence of fuels and topography on burn severity ((41, 45, 62, 63), but see e.g., (42)), our results indicate that in topographically heterogeneous, fuel-rich landscapes like the western Cascades, these fine-scale factors interact with and mediate the influence of extreme winds on fire severity during periods of extreme atmospheric and fuel aridity.

The ca. 350,000 ha that burned during the 2020 Labor Day fires represents nearly 10 times the area that burned in the western hemlock vegetation zone of the PNW between 1984–2010 (47), and matches historical (20) and modeled large burns in the region (64). More than half the 2020 burn extent occurred at high severity (> 75% mortality; Table S5), twice the high-severity proportion observed during the 1984–2010 period (47). The vast majority of the area burned over the ca. 72-hour period with extreme east winds and high fuel aridity (P1; Fig. 1), matches weather conditions reported during historic large-scale events (49, 50). Fire activity that continued once east winds subsided, yet while fuel aridity remained extreme (P2; Fig. 1), more closely resembled that extent and proportion of high-severity fire activity observed between 1984–2010 (47). Overall, the burn severity patterns found in our study area (ca. 62%) were higher than those founds among other megafire events in wet-temperate climate regions elsewhere (9, 24).

The probability of high-burn severity was substantially higher during the period of high fuel aridity with extreme winds (P1), yet lower in predictability was lower. The lower predictability is expected empirically (65) and conceptually (66) due extreme winds and stochastic fire behavior. Confirming hypothesis H1, topography (i.e., slope) was the most important predictor of high-burn severity during P1 yet became less influential than forest structure (i.e., canopy height) during P2, contrary to hypothesis H2. Although this switch in the strongest predictors of fire severity was evident when extreme winds subsided, both topographic and forest structure variables played notably important roles in driving high-severity fire during both periods. As cool air and overall fire protection returned to canyon bottoms and drainages when winds subsided (67), fire was shifted towards flatter and SW/W-facing slopes. This shift was particularly notable among the southernmost fires, which saw a greater proportion of high-severity fire along south and southwestern slopes compared to the three northern fires (Fig. S4; (20, 47, 68)). With the drop in wind speeds, slopes were less important than canopy height and stand age during P2. The probability of high-burn severity remained high for low-stature forests while taller trees were likely protected by thicker bark, increased canopy-base height (69), and lower canopy bulk density (70, 71). This buffering effect was amplified along streams in the moist, deep soils of the canyon bottom (34, 66, 72). Thus, fuel moisture patterns associated with topography (e.g., canyon bottoms and drainages) did not buffer vegetation from high-severity burns during P1 as conventionally expected (i.e., fire refugia, (66); but see (73)), and only in P2 did topographically drier south- and southwest-facing slopes experience the highest burn severity due to high afternoon solar radiation, (e.g., (74)). In summary, these results indicate that under current variability of climate and weather conditions, tall/old stands are more likely to be protected from high-severity burns outside of extreme wind events, while short stands can burn under high fuel aridity alone even on flatter areas.

Similar to fires within the drier forests east of the Cascades (75) topography interacted with the effects of fuel aridity and winds on burn severity as hypothesized. During the atmospherically arid and windy period, severity was particularly influenced by steep slopes, which were more exposed to winds, likely creating convective heating, and favoring fast fire spread (34, 72, 76). While the probability of high-burn severity was especially high on east-facing slopes, even protected canyons oriented parallel to the east winds burned at higher rates of severity than those observed during the past half-century (72, 77, 78).

Steep slopes amplified the effects of strong winds and lead to extensive mortality in taller and older stands to high-burn severity. The extent of high-severity burns within older stands during the first period of the fires suggests that winds are a key mechanism in the periodic, large-scale conflagrations that have historically marked the region (79–81).

With wildfires becoming larger and more costly (82), managers, planners, and emergency responders are challenged to understand whether ongoing extreme fire-weather conditions are likely to result in high-severity fires in the mesic, temperate forests of the PNW and elsewhere (83). Our results highlight that the early-seral, even-aged plantations burned more severely than their older and taller counterparts over the entire event of 5 combined megafires, and particularly during the period without extreme wind. The short-stature of these forests reduces thermal buffering (84) and increases ground-to-canopy connectivity, making young forests susceptible to widespread mortality (77, 85, 86). Similar results have been reported for intensively managed forests in dry and mixed-conifer forests across the western US (87), as well as in moist forests elsewhere (e.g., (88)). Broad shifts in US industrial forestry have shortened harvest rotations (89, 90), which increases the vulnerability of these forests even in the absence of extreme wind. Because timberlands in the PNW are typically closer to large, urban areas, fires in these forests have proportionally higher impacts on urban air and water supplies. Our data suggest role for both management legacies and extreme conditions of fuel aridity and wind. Wildfire managers also should be particularly alert to reburns in the mid-term future following high-severity fires (i.e., before canopy closure), as we expect increased flammability on recently burned landscapes due to growth of early seral species such as grasses and forbs that dry easily may increase rates of fire spread (e.g., (54, 91, 92)). These conditions could lead to large-scale reburns even in the absence of extreme winds, and ultimately forest conversion if tree regeneration or climate is limiting (93).

Although increased fuel aridity under climate change may prime western Cascade forests to burn more frequently and at higher severities than historically observed (94), and especially among early-seral stands (86), the difference in fire behavior between the two meteorological periods indicate that high-severity megafires are unlikely to occur without coinciding extreme wind events. Although little work has been conducted on extreme summer wind events in the PNW, increases in annual downslope wind activity have been observed in the Cascades during the 1979–2018 period (95) and global warming has been linked to severe storms and shifts in storm tracks (e.g., (96)). As climate change continues to lengthen fire seasons (97), extreme fuel aridity will extend further into late summer and early fall (4, 98), when dry east winds are more frequent (e.g., (99)). Extreme winds notwithstanding, the 2020 fire season mirrors observed climate-driven trends in increasing area burned across the western US (4, 48). Increased fire activity under extremely high fuel aridity has been projected by mid-21st century for the western Cascades (e.g., (100, 101)). Thus, even without understanding future climate influences on large scale wind events like those observed in the PNW in September 2020, chronically warmer conditions with higher fuel aridity will prime temperate mesic forests for more frequent megafires (28, 102, 103). Addressing megafires in these mesic systems may require rethinking adaptation approaches common in dry forests globally (e.g., (104–106)).

Global increases in megafires are of paramount concern to ecosystems and human well-being yet the specific mechanisms have driven this growth are not well understood. More work in the PNW, across the western US, and elsewhere (24, 30) is needed to understand large-scale and synoptic conditions that favor extreme fire behavior under warming (e.g., (76, 107–109)particularly with respect to climate-restricted fire regimes common to mesic temperate forests. Rapid climate change has and will continue to disequilibrate historical relationships between productivity gradients and burn activity (110, 111), leading to increases fire activity within fuel-rich areas where fire has historically been climate-limited. While studies show that increasing fire activity will occur in transition zones where large and continuous fuel loads are ready to burn (112), megafires events such as the 2020 Black Summer in SE Australia, the 2020 Lightning Complexes in California, and the 2020 Labor Day fires in Oregon are linked to the compounding effects of multiple switches controlling fire regimes. Debates continue in SE Australian between those that attribute the megafires to altered fuel loads tied to management legacies (61) with those that point to extreme fuel aridity (60, 113), while both likely had compounding effects. Understanding how these switches interact and fluctuate will be necessary to better understand the conditions under which these megafires are likely to form.

# 4. Methods

Wildfire severity was derived in Google Earth Engine using Sentinel-2 surface reflectance satellite images taken on September 1st (pre) and October 2nd, 2020 (post; https://developers.google.com/earth-engine/dataset). Given the temporal fire synchrony and regional homogeneity in long-term climate conditions and broad vegetation groups, we calculated burn severity as the differenced normalized burn ratio (dNBR) between pre- and post-fire images (114, 115). Continuous dNBR values were classified as a binary response variable: high-severity (>75% tree mortality; dNBR >0.44) and non-high-severity (<75% tree mortality; dNBR < 0.44; Fig. S2) fire effects, following thresholds outlined by (116, 117) in a geographically and ecologically similar study areas and our visual interpretation of the high-resolution post-fire Sentinel imagery. We also explored the use of dNBR as a continuous variable but found that the response from predictors remained the same (see Fig. S2 for comparison).

We examined the effects of six explanatory variables, which functionally represent widely used fuel structure and topographic drivers of burn severity (e.g., (34, 64)). Forest fuel structure variables included stand age and canopy height and topographic variables included slope, aspect, the heat load index (HLI), and the topographic wetness index (TWI). Although the HLI and TWI indices are calculated from topographic variables (e.g., slope, aspect, latitude), they are also correlated with forest structure legacies in the Cascades ((54) and thus, may be interpreted as proxies for topographic microclimate that also capture biotic-abiotic interactions (118). Specifically, the HLI describes evapotranspiration potential, or the relative dryness/wetness of a location based on annual incident solar radiation (119), while the TWI describes the steady-state effect of topography on runoff flow direction and accumulation, and therefore soil and microclimatic moisture availability to vegetation (120).

Given the focus of this study on upland forests in the western Cascades, we removed 14.6% of the area within the selected fire perimeters (Table S1), including (1) areas not classified as upland forest or woodland (2.9%), (2) areas east of the Cascade crest divide (4.3%), (3) land not owned by the Forest Service, Bureau of Land Management (BLM), state, or private (10.9%). To distinguish forests between the two weather periods, burned areas were geographically divided into two categories based on the first day Suomi NPP satellite's 375m VIIRS sensor-detected fire activity (i.e., September 7-9 extreme winds and fuel aridity event vs. September 10-17 mild winds and extreme fuel aridity). Land within the perimeter where fire was not observed by the VIIRS sensor was also removed (1.6 %).

Topographic variables were calculated from a 90m digital elevation model derived from LANDFIRE. Forest fuel structure variables were extracted from the LANDFIRE 2.0 remap (circa 2016; also see (121)) and the 2012 LEMMA GNN dataset at 30m spatial resolutions (122). All 30m resolution datasets were aggregated to 90m to reduce processing time and capture patterns at a spatial grain appropriate for coarse-scale analyses. To account for potential changes in forest structure post-2012, we used annual forest loss data via (123) to update the LEMMA forest age variable to 2020 conditions (i.e., in severely disturbed forests, age was set back to zero in the year a disturbance occurred). To ensure LANDFIRE forest fuel structure variables matched 2020 pre-fire conditions, annual forest loss data was also used to remove areas that experienced forest loss post-2016 from the study (5.8%). After all data filters had been applied, we retained 86% of the total area within all five fire perimeters for analyses.

We used logistic boosted regression trees (BRT) fit with a Bernoulli error distribution to model high-severity wildfire as a binary response across the five combined fire perimeters. One model was fit on the entire burn period and two other models were fit separately under extreme (P1) and the following mild (P2) wind conditions. We fit two final BRT models on burned areas stratified by P1 and P2 using the same six variables: slope, aspect, the heat load index (HLI), the topographic wetness index (TWI), forest stand age, and canopy height (CH). To evaluate model performance, we relied on the receiver operator characteristic area under the curve (AUC-ROC) from the cross-validation samples across the two burn-weather periods. AUC of the BRTs during P1 (ensemble BRTs) was 0.675 (SD = 0.005) and 0.710 during P2 (single BRT).

For P1, burn severity was calculated from an ensemble of 50 boosted regression trees each fit on a sample of 10,000 points across all fires, which were drawn randomly from a 90m grid to avoid spatial autocorrelation. Uncertainty in response was estimated for P1 dependence plots by plotting trends for the 10%, 50%, and 90th quantile values at regular intervals along the X-axis. Fitting an ensemble of BRT on repeated subsamples showed a high degree of consistency in modeled severity response that due to sample size (burn area) was only feasible during P1, which suggests that the relationships observed between most predictors and probability of high burn severity were highly significant but also weak absolute predictors of fire severity at any single location. Partial dependencies (PDs) for the P2 response were estimated separately as a single response curve owing to the fewer observations. The partial dependence (PD) of burn severity was calculated for both P1 and P2 and describes the likelihood of high severity across the observed range for a given predictive variable. Given that one-way PDs do not reveal

interactions with other response variables, we also examined the interaction on the probability of high-severity fire between all response variable pairs and highlighted those that had the greatest degree of interaction.

Finally, to determine how high-severity fire extent varied proportionally by land ownership and dominant forest fuel structures within, a spatial overlay approach was conducted (42, 124). Contingency tables were calculated for the observed area burned at high-severity by categories of forest structure (canopy height class), land ownership, and burn weather period. Observed burned areas (at high-severity) were separately compared with expected areas in each ownership category and canopy height class, which is proportional to the total area burned (i.e., all severities) in each land ownership category and canopy height class, respectively. Our spatial overlays assessed entire populations and not just samples. Thus, all deviations between observed and expected are viewed as real differences between the datasets and statistical tests are not necessary. However, given that our spatial datasets may exhibit minor-to-moderate classification errors that vary with spatial grain as well as forest cover type (121, 122), conservatively assume that only differences greater than ~15% would be ecologically meaningful (124).

## Declarations

# Acknowledgements

We thank Thomas Veblen, Alan Tepley, and Bart Johnson for their assistance in reviewing early versions of this manuscript and providing critical feedback in terms of organization and content. Partial funding for this work was provided through the National Science Foundation CNH2L Grant #1922866 and the US Forest Service Award # 20-JV-11221637-062

## References

1. Bowman, D. M. J. S. *et al.* Vegetation fires in the Anthropocene. *Nat Rev Earth Environ*, **1**, 500–515 (2020).
2. Cattau, M. E., Wessman, C., Mahood, A. & Balch, J. K. Anthropogenic and lightning-started fires are becoming larger and more frequent over a longer season length in the U.S.A. *Global Ecol Biogeogr*, **29**, 668–681 (2020).
3. Khorshidi, M. S. *et al.* Increasing concurrence of wildfire drivers tripled megafire critical danger days in Southern California between1982 and 2018. *Environ Res Lett*, **15**, 104002 (2020).
4. Abatzoglou, J. T. & Williams, P. A. Impact of anthropogenic climate change on wildfire across western US forests. Proceedings of the National Academy of Sciences 113, 11770–11775(2016).
5. Balch, J. K. *et al.* Human-started wildfires expand the fire niche across the United States. Proceedings of the National Academy of Sciences 114, 2946–2951(2017).
6. Haugo, R. D. *et al.* The missing fire: quantifying human exclusion of wildfire in Pacific Northwest forests. *USA. Ecosphere*, **10**, e02702 (2019).

7. Keane, R. E. Cascading effects of fire exclusion in Rocky Mountain ecosystems: a literature review(2002).
8. Marlon, J. *et al.* Wildfire responses to abrupt climate change in North America. Proceedings of the National Academy of Sciences 106, 2519–2524(2009).
9. Xu, W., He, H. S., Hawbaker, T. J., Zhu, Z. & Henne, P. D. Estimating burn severity and carbon emissions from a historic megafire in boreal forests of China. *Sci Total Environ*, **716**, 136534 (2020).
10. Gleason, K. E., McConnell, J. R., Arienzo, M. M., Chellman, N. & Calvin, W. M. Four-fold increase in solar forcing on snow in western U.S. burned forests since 1999. *Nat Commun*, **10**, 2026 (2019).
11. de la Barrera, F., Barraza, F., Favier, P., Ruiz, V. & Quense, J. Megafires in Chile 2017: Monitoring multiscale environmental impacts of burned ecosystems. *Sci Total Environ*, **637**, 1526–1536 (2018).
12. Jones, G. M. *et al.* Megafires: an emerging threat to old-forest species. *Front Ecol Environ*, **14**, 300–306 (2016).
13. Littell, J. S. Drought and Fire in the Western USA: Is Climate Attribution Enough? *Current Climate Change Reports*, **4**, 396–406 (2018).
14. Mariani, M. *et al.* Climate Change Amplifications of Climate-Fire Teleconnections in the Southern Hemisphere. *Geophys Res Lett*, **45**, 5071–5081 (2018).
15. McKenzie, D. & Littell, J. S. Climate change and the eco-hydrology of fire: Will area burned increase in a warming western USA? *Ecological applications: a publication of the Ecological Society of America*, **27**, 26–36 (2017).
16. Sommerfeld, A. *et al.* Patterns and drivers of recent disturbances across the temperate forest biome. *Nature Communications*, **9**, 4355 (2018).
17. Agee, J. K. *Fire ecology of Pacific Northwest forests* (Island press, 1996).
18. Baker, W. L. *Fire ecology in Rocky Mountain landscapes* (Island Press, 2009).
19. Gavin, D. G., Brubaker, L. B., Lertzman, K. P. & HOLOCENE FIRE HISTORY OF A COASTAL TEMPERATE RAIN FOREST BASED ON SOIL CHARCOAL RADIOCARBON DATES., **84**, 186–201 (2003).
20. Spies, T. A. *et al. Chapter 3: Old Growth, Disturbance, Forest Succession, and Management in the Area of the Northwest Forest Plan* (S Department of Agriculture, Forest Service, Pacific Northwest Research Station, 2018).
21. Walsh, M. K., Marlon, J. R., Goring, S. J., Brown, K. J. & Gavin, D. G. A Regional Perspective on Holocene Fire–Climate–Human Interactions in the Pacific Northwest of North America. *Ann Assoc Am Geogr*, **105**, 1135–1157 (2015).
22. Tepley, A. J., Swanson, F. J. & Spies, T. A. Fire-mediated pathways of stand development in Douglas-fir/western hemlock forests of the Pacific Northwest. *USA. Ecology*, **94**, 1729–1743 (2013).
23. Bradstock, R. A., Hammill, K. A., Collins, L. & Price, O. Effects of weather, fuel and terrain on fire severity in topographically diverse landscapes of south-eastern Australia. *Landscape Ecol*, **25**, 607–619 (2010).

24. Collins, L. *et al.* The 2019/2020 mega-fires exposed Australian ecosystems to an unprecedented extent of high-severity fire. *Environ Res Lett*, **16**, 044029 (2021).
25. DellaSala, D. A. *Temperate and boreal rainforests of the world: ecology and conservation* (Island Press, 2011).
26. Duane, A., Castellnou, M. & Brotons, L. Towards a comprehensive look at global drivers of novel extreme wildfire events. *Clim. Change*, **165**, 43 (2021).
27. Keith, H., Mackey, B. G. & Lindenmayer, D. B. Re-evaluation of forest biomass carbon stocks and lessons from the world's most carbon-dense forests. *Proc National Acad Sci*, **106**, 11635–11640 (2009).
28. Halofsky, J. S. *et al.* The nature of the beast: examining climate adaptation options in forests with stand-replacing fire regimes. *Ecosphere*, **9**, e02140 (2018).
29. Donato, D. C., Halofsky, J. S. & Reilly, M. J. Corralling a black swan: natural range of variation in a forest landscape driven by rare, extreme events.*Ecol Appl***30** (2020).
30. Boer, M. M., de Dios, V. R. & Bradstock, R. A. Unprecedented burn area of Australian mega forest fires. *Nat Clim Change*, **10**, 171–172 (2020).
31. Parks, S. A. *et al.* How will climate change affect wildland fire severity in the western US? *Environmental Research Letters*, **11**, 035002 (2016).
32. McWethy, D. B. *et al.* Landscape drivers of recent fire activity (2001–2017) in south-central Chile., **13**, e0201195 (2018).
33. Parisien, M. A. *et al.* Fire deficit increases wildfire risk for many communities in the Canadian boreal forest. *Nat Commun*, **11**, 2121 (2020).
34. Bradstock, R. A. A biogeographic model of fire regimes in Australia: current and future implications. *Global Ecol Biogeogr*, **19**, 145–158 (2010).
35. McWethy, D. *et al.* A conceptual framework for predicting temperate ecosystem sensitivity to human impacts on fire regimes. *Global Ecology and Biogeography*, **22**, 900–912 (2013).
36. Weisberg, P. J. & Swanson, F. J. Regional synchroneity in fire regimes of western Oregon and Washington, USA. *Forest Ecol Manag*, **172**, 17–28 (2003).
37. Moritz, M. A. *et al.* Climate change and disruptions to global fire activity. *Ecosphere*, **3**, 1–22 (2012).
38. Abatzoglou, J. T., Rupp, D. E., O'Neill, L. W. & Sadegh, M. Compound Extremes Drive the Western Oregon Wildfires of September 2020.*Geophys Res Lett***48** (2021).
39. Turner, M. G., Romme, W. H., Gardner, R. H., O'Neill, R. V. & Kratz, T. K. A revised concept of landscape equilibrium: Disturbance and stability on scaled landscapes. *Landscape Ecol*, **8**, 213–227 (1993).
40. McKenzie, D. & Kennedy, M. C. Power laws reveal phase transitions in landscape controls of fire regimes. *Nat Commun*, **3**, 726 (2012).
41. Bessie, W. C. & Johnson, E. A. The Relative Importance of Fuels and Weather on Fire Behavior in Subalpine Forests., **76**, 747–762 (1995).

42. Bigler, C., Kulakowski, D. & Veblen, T. T. Multiple Disturbance Interactions and Drought Influence Fire Severity in Rocky Mountain Subalpine Forests., **86**, 3018–3029 (2005).
43. Thompson, J. R. & Spies, T. A. Vegetation and weather explain variation in crown damage within a large mixed-severity wildfire. *Forest Ecol Manag*, **258**, 1684–1694 (2009).
44. Agee, J. K. The Landscape Ecology of Western Forest Fire Regimes.*Northwest Science*(1998).
45. Turner, M. G. & Romme, W. H. Landscape dynamics in crown fire ecosystems. *Landscape Ecol*, **9**, 59–77 (1994).
46. Walker, X. J. *et al.* Fuel availability not fire weather controls boreal wildfire severity and carbon emissions. *Nat Clim Change*, **10**, 1130–1136 (2020).
47. Reilly, M. J. *et al.* Contemporary patterns of fire extent and severity in forests of the Pacific Northwest, USA (1985–2010). *Ecosphere*, **8**, e01695 (2017).
48. Higuera, P. E. & Abatzoglou, J. T. Record-setting climate enabled the extraordinary 2020 fire season in the western United States. *Global Change Biol*, **27**, 1–2 (2021).
49. Morris, W. G. Forest Fires in Western Oregon and Western Washington. *Oregon Historical Quarterly*, **35**, 313–339 (1934).
50. Dague, C. I. The Weather of the Great Tillamook, Oreg., Fire in August 1933. *Mon Weather Rev*, **62**, 227–231 (1934).
51. Cramer, O. P. *Dry East Winds Over Northwest Oregon and Wouthwest Washington* (Pacific Northwest Forest & Range Experiment Station, 1957).
52. Agee, J. K. & Skinner, C. N. Basic principles of forest fuel reduction treatments. *Forest Ecology and Management*, **211**, 83–96 (2005).
53. Cartwright, J. Landscape Topoedaphic Features Create Refugia from Drought and Insect Disturbance in a Lodgepole and Whitebark Pine Forest. *Forests*, **9**, 715 (2018).
54. Busby, S. U., Moffett, K. B. & Holz, A. High-severity and short-interval wildfires limit forest recovery in the Central Cascade Range.*Ecosphere***11** (2020).
55. Nyman, P., Baillie, C. C., Duff, T. J. & Sheridan, G. J. Eco-hydrological controls on microclimate and surface fuel evaporation in complex terrain. *Agr Forest Meteorol*, **252**, 49–61 (2018).
56. Jones, M. W. *et al.* Climate Change Increases the Risk of Wildfires. *ScienceBrief Review*, **116**, 117 (2020).
57. UNEP, Are “megafires” the new normal? (2020) (December 1, 2020).
58. Heyerdahl, E. K., Brubaker, L. B. & Agee, J. K. Spatial Controls of Historical Fire Regimes: A Multiscale Example from the Interior West, USA., **82**, 660–678 (2001).
59. Keeley, J. E. & Syphard, A. D. Twenty-first century California, USA, wildfires: fuel-dominated vs. wind-dominated fires. *Fire Ecol*, **15**, 24 (2019).
60. Nolan, R. H. *et al.* Causes and consequences of eastern Australia’s 2019–20 season of mega-fires. *Global Change Biol*, **26**, 1039–1041 (2020).

61. Adams, M. A., Shadmanroodposhti, M. & Neumann, M. Causes and consequences of Eastern Australia's 2019–20 season of mega-fires: A broader perspective. *Global Change Biol*, **26**, 3756–3758 (2020).
62. Dillon, G. K. *et al.* Both topography and climate affected forest and woodland burn severity in two regions of the western US, 1984 to 2006. *Ecosphere*, **2**, 1–33 (2011).
63. Parks, S. A., Parisien, M. A., Miller, C. & Dobrowski, S. Z. Fire Activity and Severity in the Western US Vary along Proxy Gradients Representing Fuel Amount and Fuel Moisture. *PLoS ONE*, **9**, e99699 (2014).
64. Parks, S. A. *et al.* High-severity fire: evaluating its key drivers and mapping its probability across western US forests. *Environ Res Lett*, **13**, 044037 (2018).
65. Povak, N. A., Kane, V. R., Collins, B. M., Lydersen, J. M. & Kane, J. T. Multi-scaled drivers of severity patterns vary across land ownerships for the 2013 Rim Fire, California. *Landscape Ecol*, **35**, 293–318 (2020).
66. Krawchuk, M. A. *et al.* Topographic and fire weather controls of fire refugia in forested ecosystems of northwestern North America.*Ecosphere***7** (2016).
67. Dobrowski, S. Z. A climatic basis for microrefugia: the influence of terrain on climate. *Global Change Biol*, **17**, 1022–1035 (2011).
68. Littell, J. S., Peterson, D. L., Riley, K. L., Liu, Y. & Luce, C. H. A review of the relationships between drought and forest fire in the United States. *Global change biology*, **22**, 2353–2369 (2016).
69. Lentile, L. B. *et al.* Remote sensing techniques to assess active fire characteristics and post-fire effects. *Int J Wildland Fire*, **15**, 319–345 (2006).
70. *A mathematical model for predicting fire spread in wildland fuels* (Intermountain Forest & Range Experiment Station, Forest Service, US …
71. Keane, R. E., Reinhardt, E. D., Scott, J., Gray, K. & Reardon, J. Estimating forest canopy bulk density using six indirect methods. *Can J Forest Res*, **35**, 724–739 (2005).
72. Estes, B. L., Knapp, E. E., Skinner, C. N., Miller, J. D. & Preisler, H. K. Factors influencing fire severity under moderate burning conditions in the Klamath Mountains, northern California, USA. *Ecosphere*, **8**, e01794 (2017).
73. Tollefson, J. E., Swanson, F. & Cissel, J. H. Fire severity in intermittent stream drainages, Western Cascade Range, Oregon. *Northwest Science*, **78**, 186–191 (2004).
74. Taylor, A. H. & Skinner, C. N. Fire history and landscape dynamics in a late-successional reserve, Klamath Mountains, California, USA. *Forest Ecol Manag*, **111**, 285–301 (1998).
75. Cansler, C. A. & McKenzie, D. Climate, fire size, and biophysical setting control fire severity and spatial pattern in the northern Cascade Range, USA. *Ecol Appl*, **24**, 1037–1056 (2014).
76. Coen, J. L. & Stavros, E. N. J. A. Fites-Kaufman, Deconstructing the King megafire. *Ecol Appl*, **28**, 1565–1580 (2018).

77. Weatherspoon, C. P. & Skinner, C. N. An assessment of factors associated with damage to tree crowns from the 1987 wildfires in northern California. *Forest Science*, **41**, 430–451 (1995).
78. Wood, S. W., Murphy, B. P. & Bowman, D. Firescape ecology: how topography determines the contrasting distribution of fire and rain forest in the south-west of the Tasmanian Wilderness World Heritage Area. *Journal of Biogeography*, **38**, 1807–1820 (2011).
79. Agee, J. K. & Huff, M. H. Fuel succession in a western hemlock/Douglas-fir forest. *Can J Forest Res*, **17**, 697–704 (1987).
80. Franklin, J. F. *et al.* Disturbances and structural development of natural forest ecosystems with silvicultural implications, using Douglas-fir forests as an example. *Forest Ecol Manag*, **155**, 399–423 (2002).
81. Spies, T. A., Franklin, J. F. & Thomas, T. B. Coarse Woody Debris in Douglas-Fir Forests of Western Oregon and Washington., **69**, 1689–1702 (1988).
82. North, M. *et al.* Reform forest fire management., **349**, 1280–1281 (2015).
83. Williams, J. Exploring the onset of high-impact mega-fires through a forest land management prism. *Forest Ecology and Management*, **294**, 4–10 (2013).
84. Frey, S. J. K. *et al.* Spatial models reveal the microclimatic buffering capacity of old-growth forests. *Sci Adv*, **2**, e1501392 (2016).
85. Thompson, J. R. *et al.* Scenario Studies as a Synthetic and Integrative Research Activity for Long-Term Ecological Research. *BioScience*, **63**, 367–376 (2012).
86. Zald, H. S. J. & Dunn, C. J. Severe fire weather and intensive forest management increase fire severity in a multi-ownership landscape. *Ecol Appl*, **28**, 1068–1080 (2018).
87. Bradley, C. M., Hanson, C. T. & DellaSala, D. A. Does increased forest protection correspond to higher fire severity in frequent-fire forests of the western United States?*Ecosphere***7** (2016).
88. Lindenmayer, D. B., Kooyman, R. M., Taylor, C., Ward, M. & Watson, J. E. M. Recent Australian wildfires made worse by logging and associated forest management. *Nat Ecol Evol*, **4**, 898–900 (2020).
89. Gunnoe, A. & The Financialization of the US Forest Products Industry. Socio-Economic Relations, Shareholder Value, and the Restructuring of an Industry. *Soc Forces*, **94**, 1075–1101 (2015).
90. Bliss, J. C., Kelly, E., Abrams, J., Bailey, C. & Dyer, J. Disintegration of the U. S. Industrial Forest Estate: Dynamics, Trajectories, and Questions. *Small-scale Forestry*, **9**, 53–66 (2010).
91. Prichard, S. J., Stevens-Rumann, C. S. & Hessburg, P. F. Tamm Review: Shifting global fire regimes: Lessons from reburns and research needs. Forest Ecology and Management 396, 217–233(2017).
92. Gray, A. N. & Franklin, J. F. Effects of multiple fires on the structure of southwestern Washington forests(1997).
93. Coop, J. D. *et al.* Wildfire-Driven Forest Conversion in Western North American Landscapes., **70**, 659–673 (2020).
94. Abatzoglou, J. T., Juang, C. S., Williams, A. P., Kolden, C. A. & Westerling, A. L. Increasing Synchronous Fire Danger in Forests of the Western United States.*Geophys Res Lett***48** (2021).

95. Abatzoglou, J. T., Hatchett, B. J., Fox-Hughes, P., Gershunov, A. & Nauslar, N. J. Global climatology of synoptically-forced downslope winds. *Int J Climatol*, **41**, 31–50 (2021).
96. Tamarin-Brodsky, T. & Kaspi, Y. Enhanced poleward propagation of storms under climate change. *Nat Geosci*, **10**, 908–913 (2017).
97. Jolly, M. W. *et al.* Climate-induced variations in global wildfire danger from 1979 to 2013. *Nature Communications*, **6**, 7537 (2015).
98. Westerling, A. Increasing western US forest wildfire activity: sensitivity to changes in the timing of spring. *Phil. Trans. R. Soc. B*, **371**, 20150178 (2016).
99. Goss, M. *et al.* Climate change is increasing the likelihood of extreme autumn wildfire conditions across California. *Environ Res Lett*, **15**, 094016 (2020).
100. Rogers, B. M. *et al.* Impacts of climate change on fire regimes and carbon stocks of the U.S. Pacific Northwest. *Journal of Geophysical Research: Biogeosciences (*2005*–2012)* **116** (2011).
101. McEvoy, A., Nielsen-Pincus, M., Holz, A., Catalano, A. J. & Gleason, K. E. Projected Impact of Mid-21st Century Climate Change on Wildfire Hazard in a Major Urban Watershed outside Portland, Oregon USA. *Fire*, **3**, 70 (2020).
102. Davis, R., Yang, Z., Yost, A., Belongie, C. & Cohen, W. The normal fire environment—Modeling environmental suitability for large forest wildfires using past, present, and future climate normals. *Forest Ecol Manag*, **390**, 173–186 (2017).
103. Halofsky, J. E., Peterson, D. L. & Harvey, B. J. Changing wildfire, changing forests: the effects of climate change on fire regimes and vegetation in the Pacific Northwest, USA. *Fire Ecol*, **16**, 4 (2020).
104. Fischer, P. A. *et al.* Wildfire risk as a socioecological pathology. *Frontiers in Ecology and the Environment*, **14**, 276–284 (2016).
105. McWethy, D. B. *et al.* Rethinking resilience to wildfire. *Nat Sustain*, **2**, 797–804 (2019).
106. Tedim, F. *et al.* Defining Extreme Wildfire Events: Difficulties, Challenges, and Impacts. *Fire*, **1**, 9 (2018).
107. Miller, N. L. & Schlegel, N. J. Climate change projected fire weather sensitivity: California Santa Ana wind occurrence.*Geophys Res Lett***33** (2006).
108. Zhang, L., Lau, W., Tao, W. & Li, Z. Large Wildfires in the Western United States Exacerbated by Tropospheric Drying Linked to a Multi-Decadal Trend in the Expansion of the Hadley Circulation.*Geophys Res Lett***47** (2020).
109. Coen, J. L., Schroeder, W., Conway, S. & Tarnay, L. Computational modeling of extreme wildland fire events: A synthesis of scientific understanding with applications to forecasting, land management, and firefighter safety. *J Comput Sci-neth*, **45**, 101152 (2020).
110. ARCHIBALD, S., ROY, D. P. & WILGEN, B. W. V. R. J. SCHOLES, What limits fire? An examination of drivers of burnt area in Southern Africa. *Global Change Biol*, **15**, 613–630 (2009).
111. Krawchuk, M. A., Moritz, M. A., Parisien, M. A., Dorn, J. & Hayhoe, K. Global Pyrogeography: the Current and Future Distribution of Wildfire. *PLoS ONE*, **4**, e5102 (2009).

112. Boer, M. M. *et al.* Changing Weather Extremes Call for Early Warning of Potential for Catastrophic Fire. *Earth's Futur*, **5**, 1196–1202 (2017).
113. Bradstock, R. A. *et al.* A broader perspective on the causes and consequences of eastern Australia's 2019–20 season of mega-fires: A response to Adams et al. *Global Change Biol*, **26**, e8–e9 (2020).
114. Miller, J. D. & Thode, A. E. Quantifying burn severity in a heterogeneous landscape with a relative version of the delta Normalized Burn Ratio (dNBR). *Remote Sens Environ*, **109**, 66–80 (2007).
115. Parks, S. A. *et al.* Giving Ecological Meaning to Satellite-Derived Fire Severity Metrics across North American Forests. *Remote Sens-basel*, **11**, 1735 (2019).
116. Key, C. H. & Benson, N. C. Landscape assessment (LA). In: Lutes, Duncan C.; Keane, Robert E.; Caratti, John F.; Key, Carl H.; Benson, Nathan C.; Sutherland, Steve; Gangi, Larry J. 2006. FIREMON: Fire effects monitoring and inventory system. Gen. Tech. Rep. RMRS-GTR-164-CD. Fort Collins, CO: US Department of Agriculture, Forest Service, Rocky Mountain Research Station. p. LA-1-55 **164** (2006).
117. Cansler, C. A. & McKenzie, D. How Robust Are Burn Severity Indices When Applied in a New Region? Evaluation of Alternate Field-Based and Remote-Sensing Methods. *Remote Sens-basel*, **4**, 456–483 (2012).
118. Countryman, C. M. *The fire environment concept* (Pacific Southwest Forest and Range Experiment Station, 1972).
119. McCune, B. & Keon, D. Equations for potential annual direct incident radiation and heat load. *J Veg Sci*, **13**, 603–606 (2002).
120. Beven, K. J. & Kirkby, M. J. A physically based, variable contributing area model of basin hydrology / Un modèle à base physique de zone d'appel variable de l'hydrologie du bassin versant. *Hydrological Sci Bulletin*, **24**, 43–69 (1979).
121. Rollins, M. G. LANDFIRE: a nationally consistent vegetation, wildland fire, and fuel assessment. *International Journal of Wildland Fire*, **18**, 235–249 (2009).
122. Ohmann, J. L., Gregory, M. J., Henderson, E. B. & Roberts, H. M. Mapping gradients of community composition with nearest-neighbour imputation: extending plot data for landscape analysis. *J Veg Sci*, **22**, 660–676 (2011).
123. Hansen, M. C. *et al.* High-Resolution Global Maps of 21st-Century Forest Cover Change., **342**, 850–853 (2013).
124. Hart, S. J., Schoennagel, T., Veblen, T. T. & Chapman, T. B. Area burned in the western United States is unaffected by recent mountain pine beetle outbreaks. *Proc National Acad Sci*, **112**, 4375–4380 (2015).

# Figures

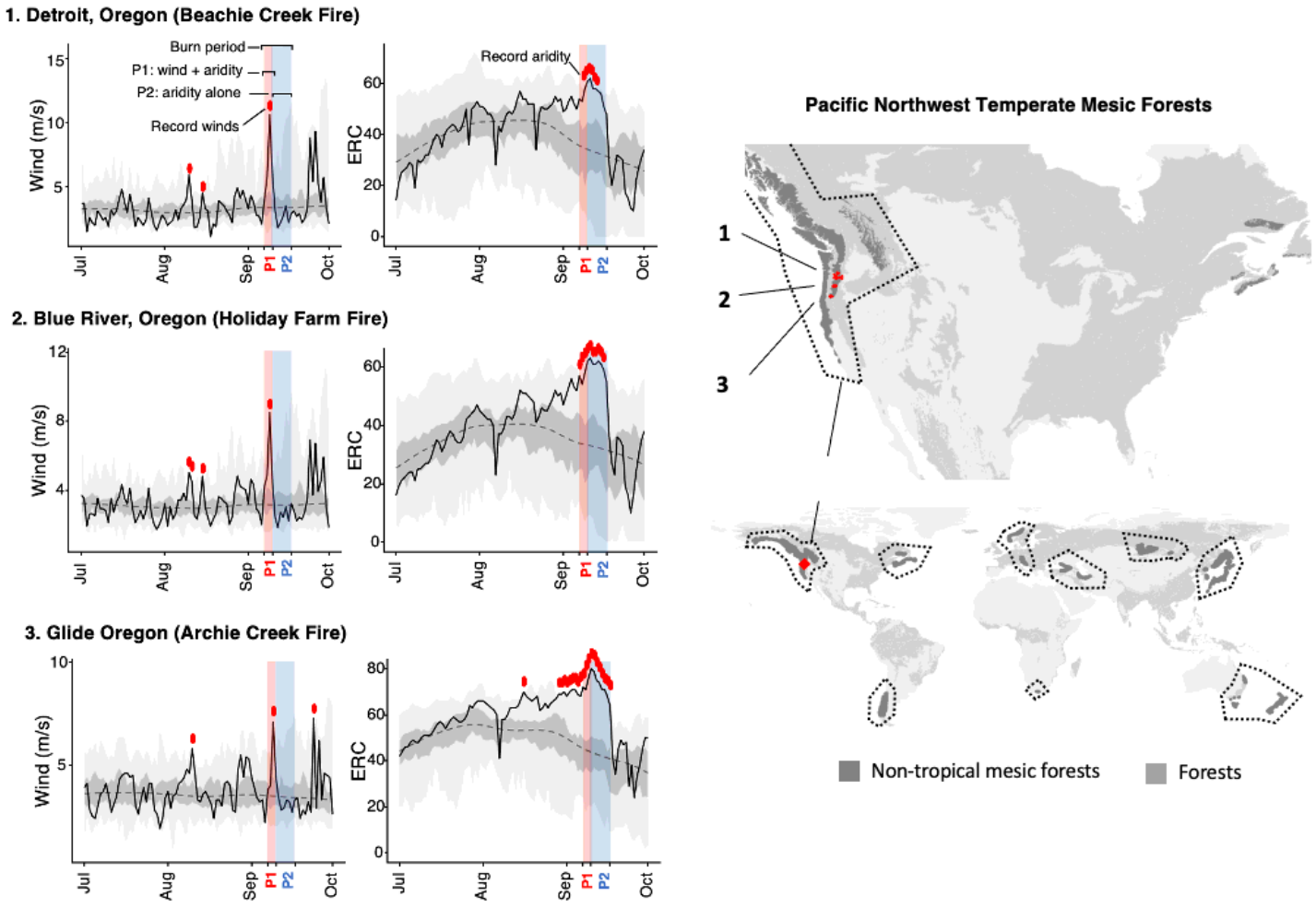


## Figure 1

Long-term (1979-2020) and 2020 weather conditions for the PNW fire season (July to Oct) from north (top panel) to south (bottom panel) in the western Cascade Range of Oregon (source: GridMET, climatologylab.org/gridmet.html). Long-term maximum daily values for wind and energy release component (ERC; a metric of mid-to-coarse fuel aridity) are shown in light grey; the interquartile range in darker grey; and the median daily value as a dashed line. 2020 daily values are shown as a solid black line (record-breaking daily values denoted with bold red emphasis). Based on wind patterns, the five synchronous megafires are divided into two periods: period 1 (P1) with extreme winds and fuel aridity (red), and period 2 (P2) with extreme fuel aridity alone (blue). From north (top) to south (bottom), the GridMET stations are located in the Santiam River watershed, near Detroit, Oregon (Beachie Creek Fire; top left panel), in the McKenzie watershed, near Blue River, Oregon (Holiday Farm Fire; middle left panel), and in the Umpqua River watershed near Glide, Oregon (Archie Creek Fire; bottom left panel). All five megafires are shown in Fig S1. The global context of these fires within temperate mesic forests is shown to the right.

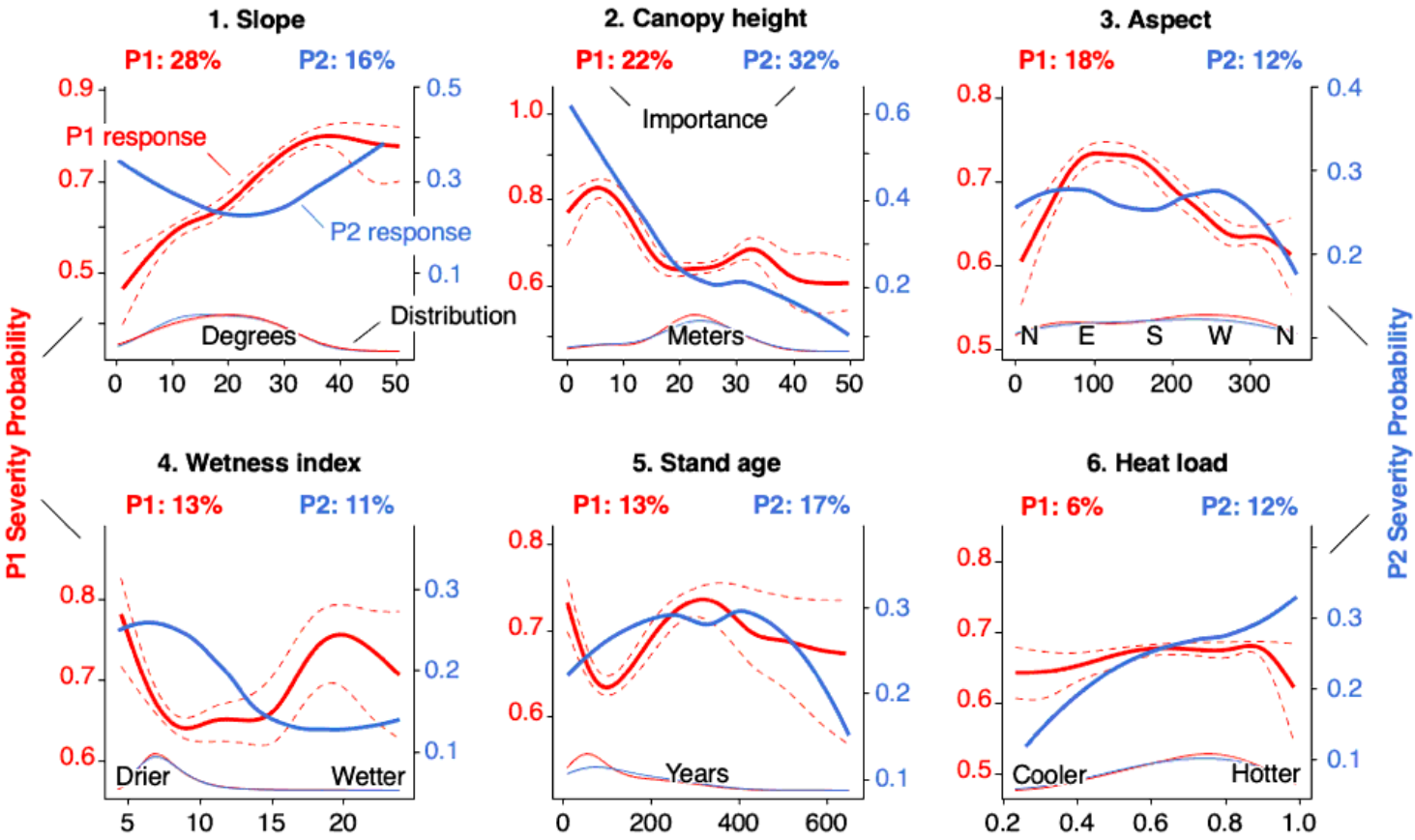


## Figure 2

Plots show the partial dependence of the probability of high-burn severity on four topographic and two fuel structure variables between the two burn-weather periods. Response during the initial extreme wind and fuel aridity period (P1) is shown in red (continuous line) as a mean across ensemble reruns with 10th and 90th percentiles (dashed lines). The following period of fuel aridity only (P2) is shown as a continuous blue line (and as a single response [run] due to the comparatively limited sample). From top-left to bottom-right panels are ordered by relative importance during P1 (% values in red) with response values specific to P1 and P2 in the panels' left and right y-axis, respectively. The relative importance of predictors during P2 is shown as % values in blue. The relative distribution of values (i.e. observed area burned) for each period is shown in gray at the bottom of each panel.

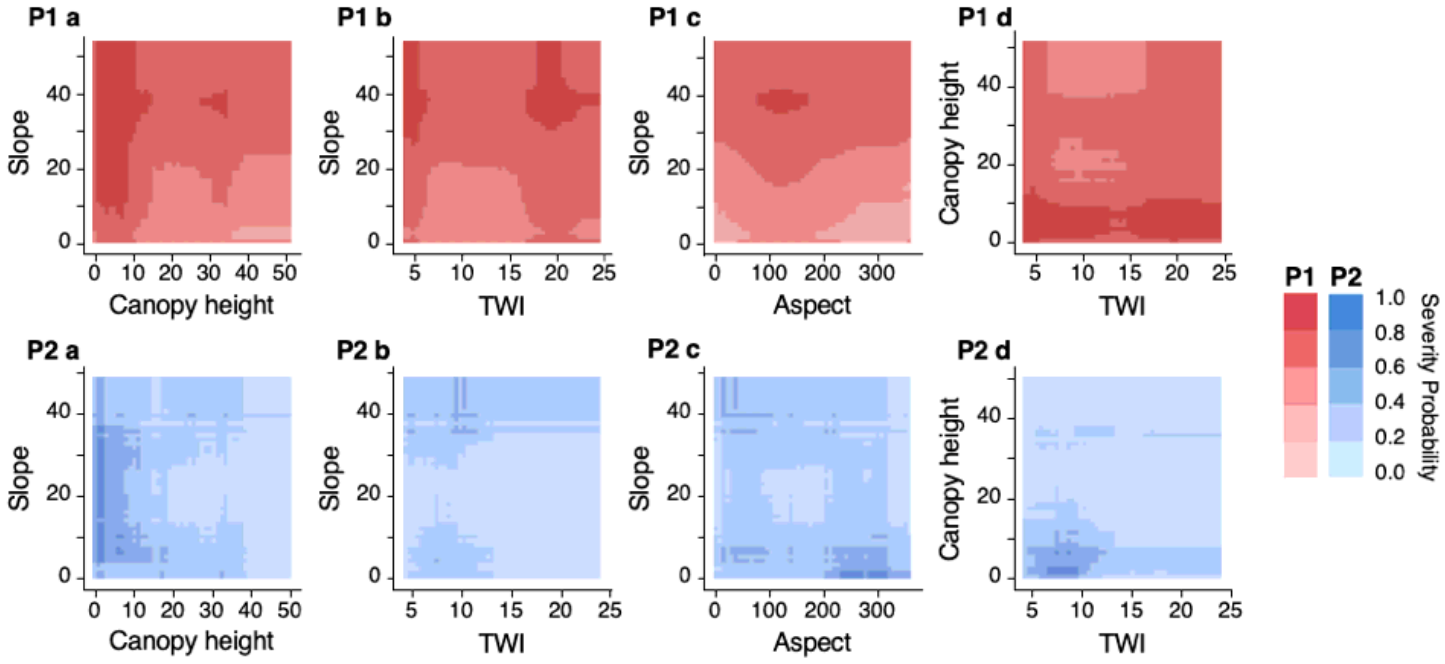


Figure 3

Interactions among the most important four variable pairs showing mean predicted response across the two burn-weather periods (P1a-d in red, and P2a-d in blue). The likelihood of a severe burn is depicted on a color-scale value-gradient for each combination of values between the pairs of explanatory variables specific to each burn period. The same four variable pairs were the strongest interactions in the models for both periods.

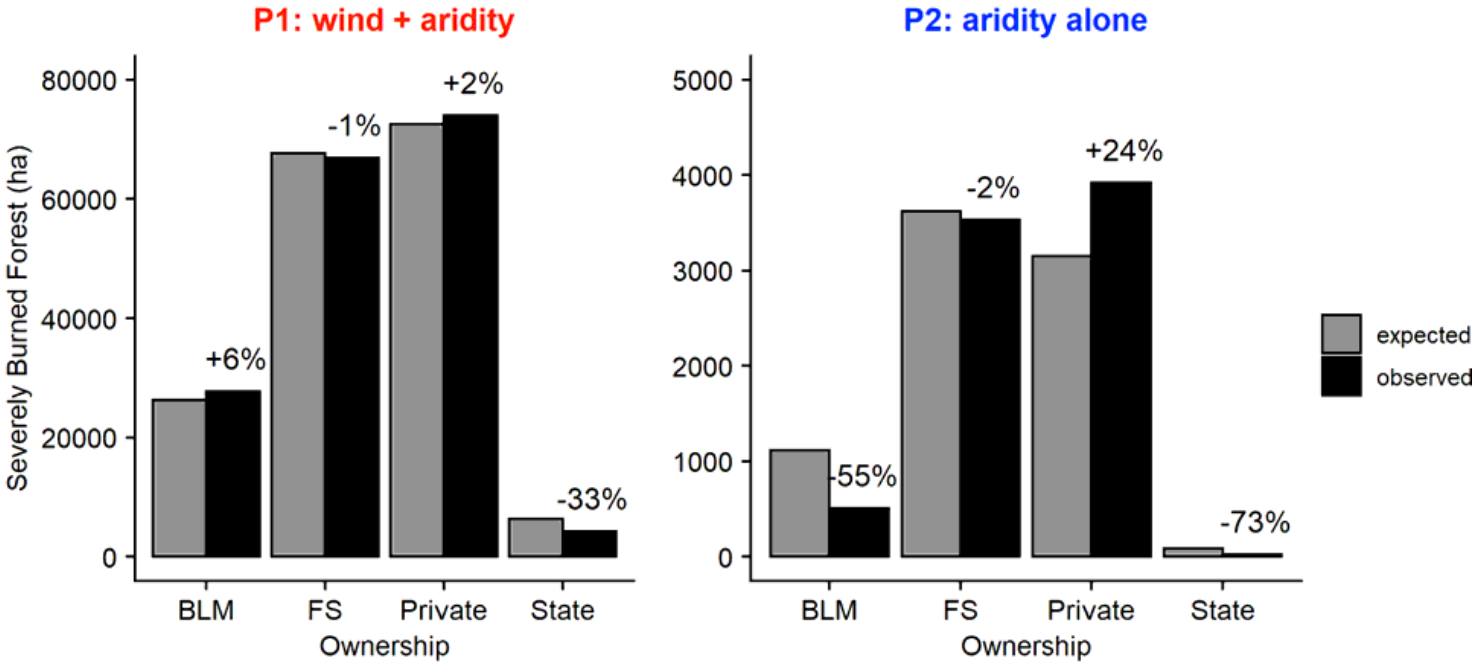


Figure 4

Expected (grey bars) and observed (black bars) areas of forest extent (hectares) burned at high severity across categories of land ownership during the two weather periods. Expected distributions were generated by calculating the proportion of the landscape in each ownership class and multiplying it by the area burned at high severity in all five burned landscapes combined. Observed distributions were generated by overlaying the area burned in each weather period with maps of land ownership as of 2020. The difference between observed and expected values is represented as the percent value located above the black bars shown above each pair of bars. Positive percentages indicate that the observed area burned was greater than expected in that ownership class. Note the difference in the y-axis scales in both panels.

## Supplementary Files

This is a list of supplementary files associated with this preprint. Click to download.

- ScientificReportsExtremeSupplementaryMaterial20210623.docx